

# DESIGN AND DEVELOPMENT OF A THERMO-IONIC ELECTRIC THRUSTOR

By Adriano C. Ducati, Erich Muehlberger and James P. Todd

Interim Report

3QS025-968

February 1965

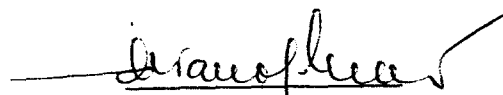
Prepared under Contract No. NAS w-968 by

GIANNINI SCIENTIFIC CORPORATION

Special Projects Group

Santa Ana, California

Approved by:



Adriano C. Ducati  
Technical Director

Prepared for:

NATIONAL AERONAUTICS AND SPACE ADMINISTRATION

Lewis Research Center

Cleveland, Ohio



## SUMMARY

29327

During the third quarterly period of this program on "Design and Development of a Thermo-Ionic Electric Thrustor" increased attention was given to investigating methods for improving thrustor performance, and experimental work which may lead to a better understanding of the operation of thermo-ionic thrustors. Work was accomplished in several areas. A scaled-down (5 KW) version of a thermo-ionic thrustor was built and tested to give an indication of the effect of scaling. Experiments have been started to determine the effect of varying magnetic field strength on thrustor performance and on the ability of the field to rotate the arc. An investigation has been initiated to determine the importance of errors in thrust measurement caused by interactions between the thrustor and the vacuum chamber gases and walls. A series of tests to evaluate propellants other than hydrogen has been started using deuterium.

## TABLE OF CONTENTS

	Page
1.0 INTRODUCTION	1
2.0 ENGINE DEVELOPMENT PROGRAM	1
2.1 The Effect of Scaling on Performance	1
2.2 The Effect of Magnetic Field Strength on Performance	3
2.3 The Effect of Magnetic Interaction on the Thrust Measurement	10
2.4 Tests With Deuterium	13
3.0 CONCLUSIONS AND RECOMMENDATIONS	20
REFERENCES	21

## LIST OF ILLUSTRATIONS

Figure		Page
1	5 KW Water-Cooled Thermo-Ionic Thrustor	2
2	5 KW Thermo-Ionic Thrustor in Operation ( $H_2$ Propellant)	5
3	Electrodes of 5 KW Thermo-Ionic Thrustor After a 2-Hour Life Test	6
4	Photograph of Various Magnetic Field Coils Used in Experimental Testing	7
5	Dimensions of Magnetic Field Coils	8
6	Cathode Heating Concept and Swirl Effect on Heated Cathode	12
7	Experimental Thermo-Ionic Thrustor With Extended Electrodes	14
8	Estimated Path of Current Discharge With Extended Electrodes at No or Weak Magnetic Field	15
9	Proposed Enlarged Test Chamber	16
10	Schematic Diagram of Dual Propellant Flow System	18

## LIST OF TABLES

Table		Page
1	Average Performance Data for the 5 KW Thermo-Ionic Thrustor	4
2	Electrical and Magnetic Properties for Various Magnetic Field Coils	9
3	Thrustor Performance Comparison at Constant Mass Flow and Different Operating Conditions	11
4	Performance Comparison of Hydrogen and Deuterium Propellants	19

## 1.0 INTRODUCTION

In the preceding report periods the experimental effort concentrated on the performance of 50-hour life tests at specific impulses ranging from 3000 to 10,000 seconds. This work was successfully completed before the start of the present report period, and results have been presented in references 1 and 2. Theoretical studies have been made in support of the experimental program; however, there still exist many unexplained factors which preclude the possibility of presenting an accurate analytical model. During the remainder of this program the primary efforts will be to evaluate alternate propellants and to discriminate between the various effects which contribute to the total thrust.

## 2.0 ENGINE DEVELOPMENT PROGRAM

In the present report period, the effort has concentrated on evaluation of the variables that affect thruster performance. The work that has been accomplished to date in this area, together with some of the testing methods which have been developed, are described in the paragraphs that follow.

### 2.1 The Effect of Scaling on Performance

To evaluate the effect of thruster size on performance, a thruster has been designed to operate at an approximate power input level of 5 KW. It may be considered as a scaled-down version of the large units used for the 50-hour life tests (these units ran at powers as high as 170 KW while operating at a specific impulse of 10,000 seconds).

Figure 1 shows the basic design configuration of this 5 KW water-cooled thermo-ionic thruster. As indicated, the throat diameter of 0.187 inch represents a cross-sectional area reduction of 25 times when compared with the average throat cross-sectional area of the large power thrusters. In this way the power density in the throat of this scaled-down thruster design was kept approximately constant. The L/D ratio of the anode throat was also kept constant. The anode consists of a water-cooled copper housing having a tungsten insert into which the throat configuration is machined. The cathode is machined from a 2 per cent thoriated tungsten rod having a diameter of 0.375 inch. The cathode in the low-power thruster was radiation-cooled. Both electrodes were designed so that they could be easily adapted to the thruster housing which had also served as the basic mount for the electrode configurations of all the thrusters used in the experimental testing under this program. In anticipation of the low current which was expected for a hydrogen jet of this power range, a larger external magnetic field coil was fabricated. As in the case of

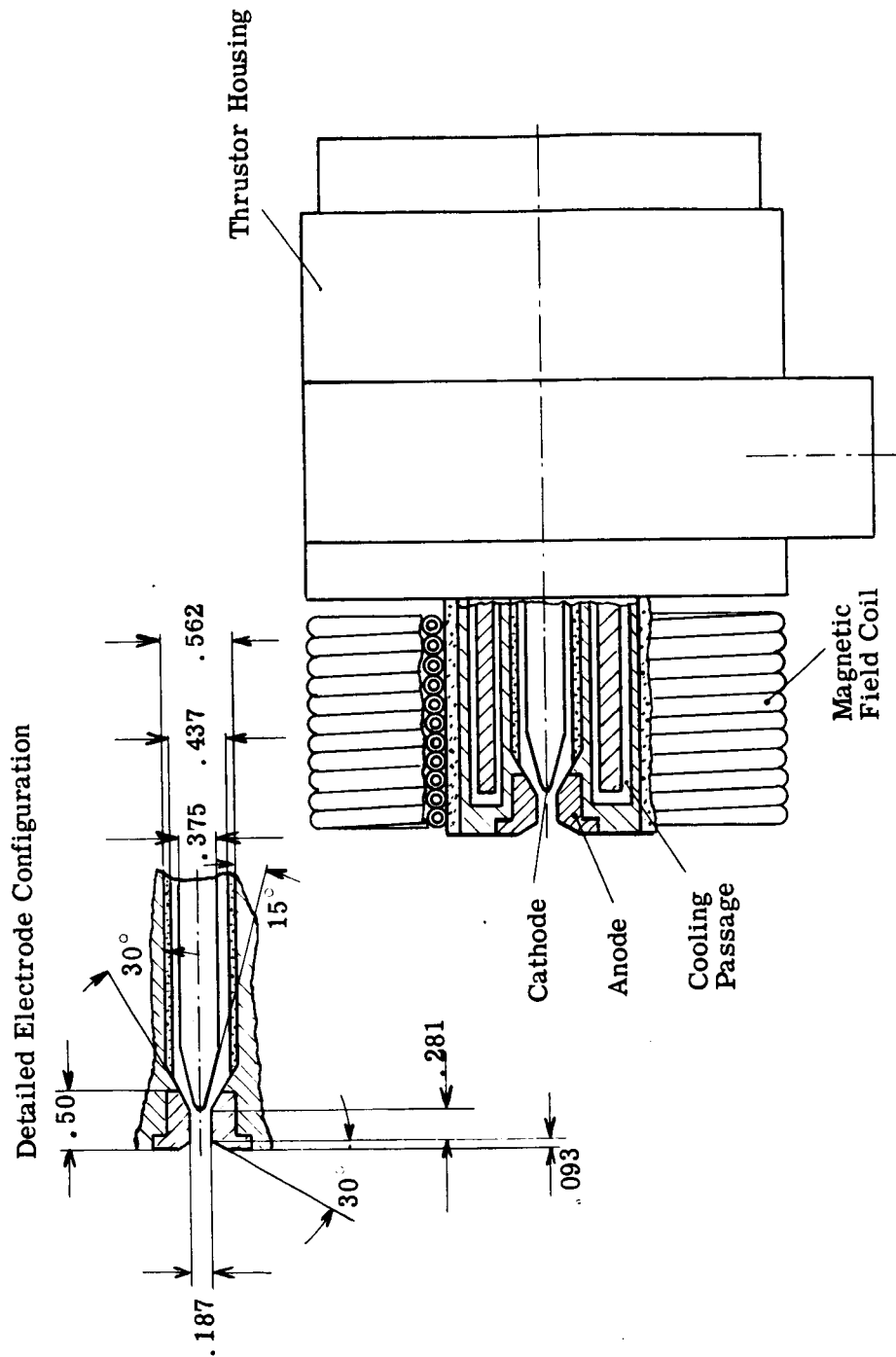


Figure 1. 5 KW Water-Cooled Thermo-Ionic Thrustor

the large thrusters, this coil was connected in series with the arc current. The magnetic field coil was designed to produce a magnetic field strength of the same order as that used with the high power thrusters for a specific impulse value of approximately 10,000 seconds, namely 2500 gauss at current values of 150 to 200 amps. The first tests indicated that the scaled-down design performed satisfactorily and the average data obtained was quite similar to that which was obtained with the 200 KW unit used during the previously reported life tests. The average performance data for a nominal Isp value of 9000 seconds is tabulated in Table 1 as it was obtained during various test runs. Figure 2 is a photograph of the thruster in operation and Figure 3 shows the good condition of the electrodes after a 2-hour test run. When compared with earlier test results of the higher power thrusters, the efficiencies  $\eta^{eg}$ ,  $\eta^{ek}$ , and  $\eta^{ek}$  are quite similar. Thus, the applied scaling method is feasible for a design of 25 times lower power, and it can be reasonably assumed that the expected lifetime of this 5 KW thruster is the same as that already demonstrated with the larger power models (see Interim Report, November 1964). This scaled-down model was intended primarily for experimental evaluation tests of thruster performance at lower ambient pressures ( $10^{-3}$  to  $10^{-4}$  mmHg). The comparatively low propellant mass flow rates used with this thruster would permit operation at these lower ambient pressure ranges with our present vacuum facilities, although some improvement on the vacuum pumps, the exhaust tank, and suction lines would be necessary.

## 2.2 The Effect of Magnetic Field Strength on Performance

A series of magnetic coils have been designed and fabricated, and a test program to permit an evaluation to be made of the effect of magnetic field strength on performance has been partially completed. It is hoped that these tests will contribute to an improved thruster design by indicating the level of magnetic field strength that results in the best performance, and by adding to the understanding of the acceleration process in thermo-ionic thrusters.

Figure 4 is a photograph of the coils used, while Figure 5 shows their primary geometric dimensions. The coils are constructed of heavy walled copper tubing (of identical size) to keep the power loss to a minimum. Table 2 summarizes the electrical and magnetic properties of the coils. The tabulated values of power loss and magnetic field strength were inferred from a series of measurements on each coil. Magnetic field strength was measured at the center of the coils. A comparison of these tabulated values with the currents measured during tests shows that field strength as high as 4500 gauss have been used during the thruster tests which have been completed so far. These coils (and the coils used earlier in this program) were all connected in series with the arc. This was done because, at present, the thrust stand doesn't have secondary power leads capable of handling the necessary current.



TABLE 1

AVERAGE PERFORMANCE DATA FOR THE  
5 KW THERMO-IONIC THRUSTOR

CONFIGURATION:

Model: C-1-1-H (water-cooled)

Propellant: Hydrogen

PERFORMANCE:

Propellant Flow Rate	0.50	mg/sec
Total Input Power (arc)	5.2	kilowatts
Coil Power	1.4	kilowatts
Arc Voltage	37.2	volts DC
Arc Current	140	amps
Thrust (measured)	4.55	grams
Specific Impulse	9100	seconds
Thrustor Efficiencies:		
Overall (electric/kinetic) incl. coil	30	%
Overall (electric/kinetic)	39	%
Thermal (electric/gas)	63	%
Kinetic (gas/kinetic)	61	%
Arc Chamber Pressure	6.1	mmHg abs.
Test Chamber Pressure	0.15	mmHg abs.

REMARKS:

Total Test Time = 2.0 hours

Total Electrode weight loss = 20 mg.

Anode = - 25 mg.

Cathode = + 5 mg.

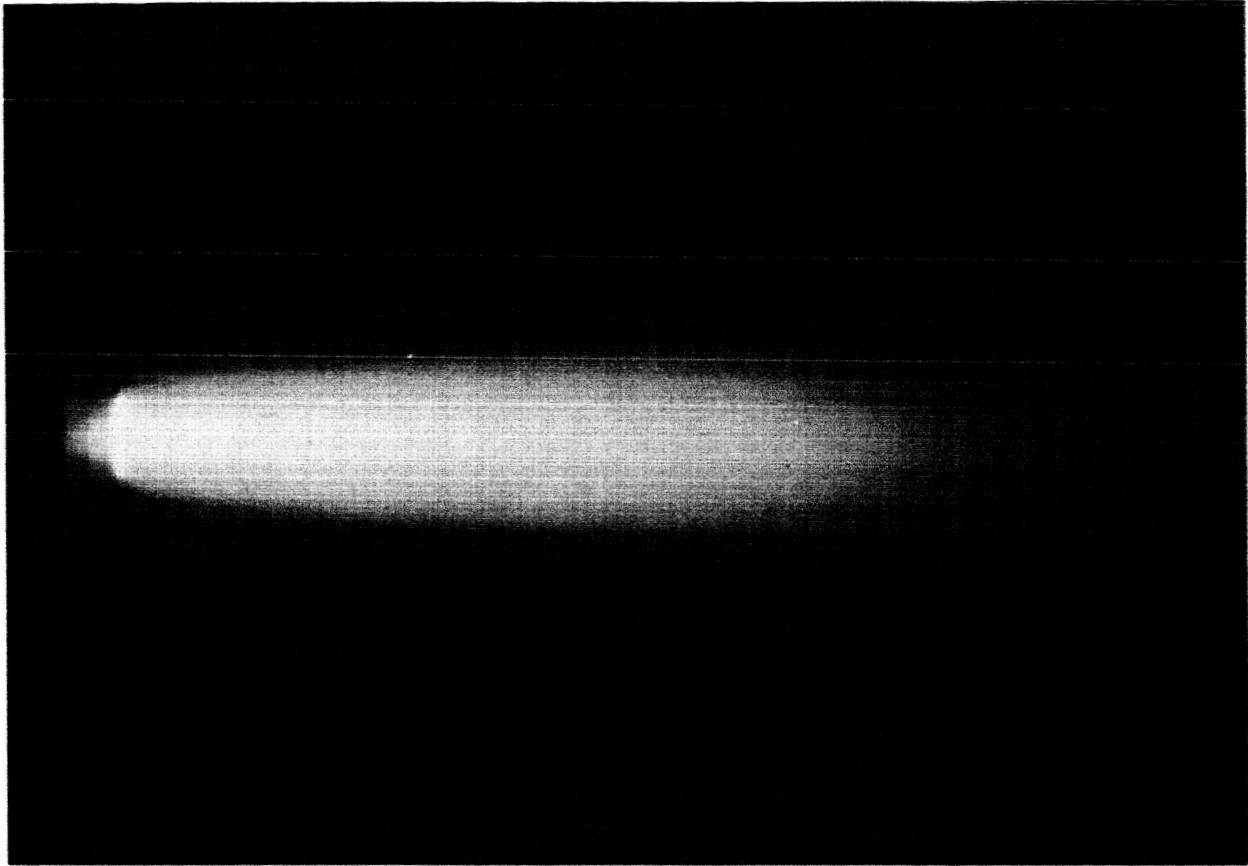


Figure 2. 5 KW Thermo-Ionic Thruster in Operation ( $H_2$  Propellant)

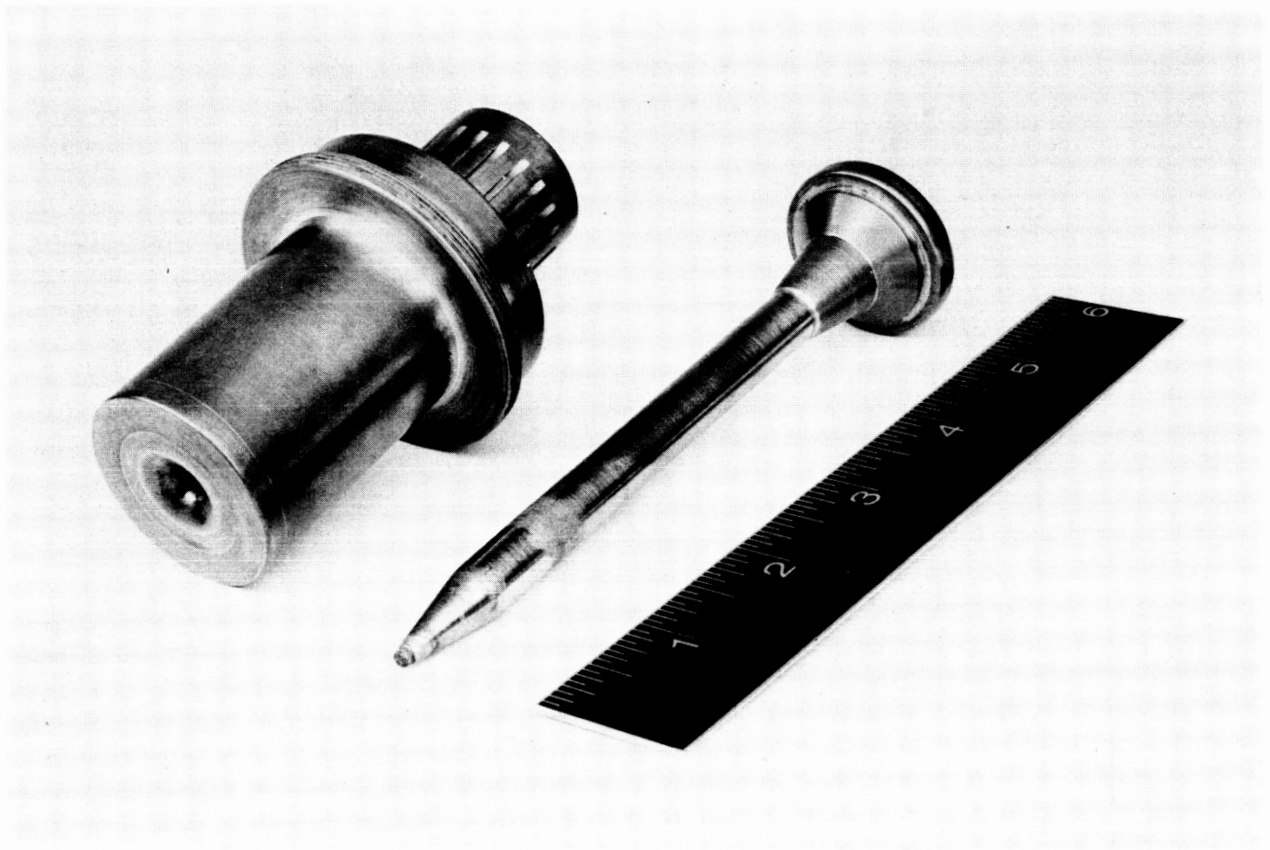


Figure 3. Electrodes of 5 KW Thermo-Ionic Thrustor After a 2-Hour Life Test

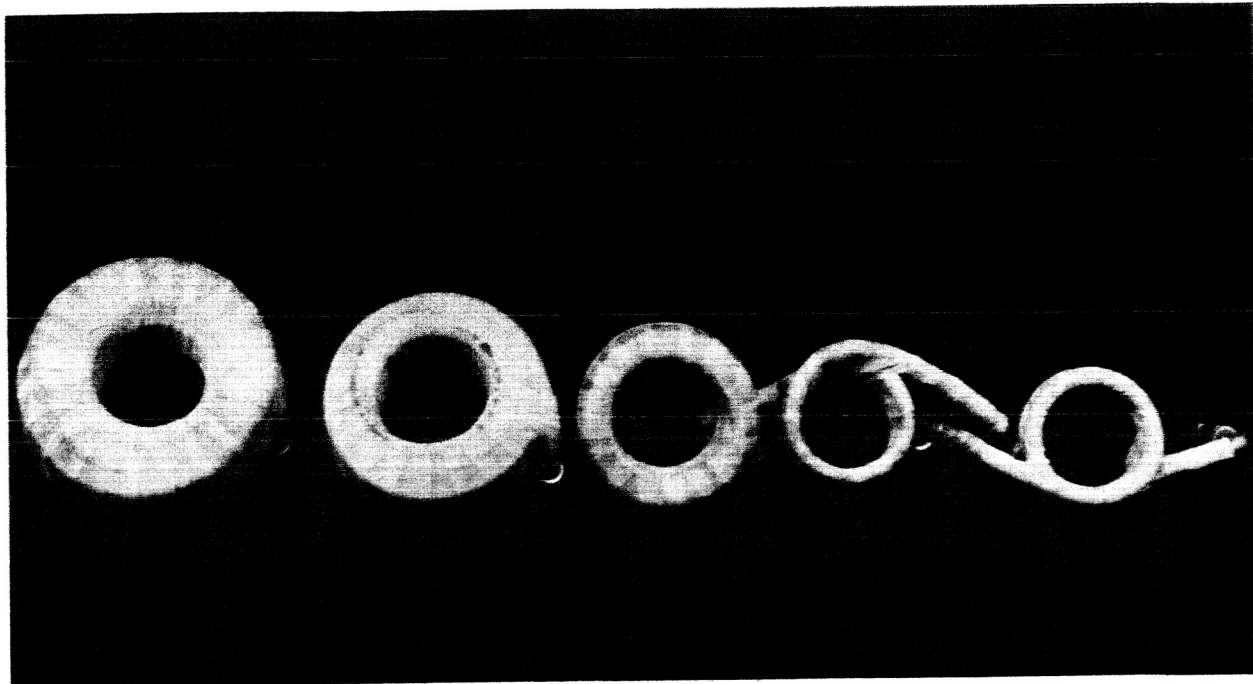
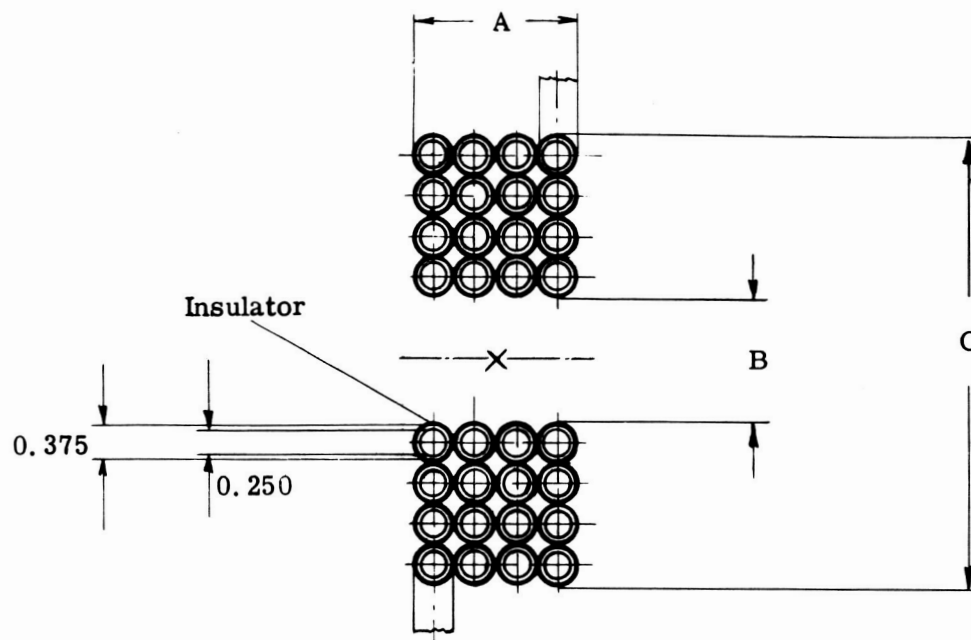


Figure 4. Photograph of Various Magnetic Field Coils Used in Experimental Testing



Coil Number Turns		2	4	8	12	16
Number of Layers		1	1	2	3	4
Length, Inches	A	0.775	1.55	1.55	1.55	1.55
Inside Diameter	B	2.250	2.250	2.250	2.250	2.250
Outside Diameter	C	3.000	3.000	3.834	4.668	5.500

Figure 5. Dimensions of Magnetic Field Coils

TABLE 2

## ELECTRICAL AND MAGNETIC PROPERTIES FOR VARIOUS MAGNETIC FIELD COILS

Coil Turns	2		4		8		12		16	
Amps	Max. Field Gauss	Power Loss KW	Max. Field Gauss	Power Loss KW	Max. Field Gauss	Power Loss KW	Max. Field Gauss	Power Loss KW	Max. Field Gauss	Power Loss KW
100	70	.007	100	.007	150	.012	225	.021	242	.029
200	130	.015	200	.028	295	.050	440	.084	475	.116
300	195	.034	285	.063	440	.114	625	.189	700	.261
400	260	.060	380	.113	580	.203	875	.337	940	.465
500	320	.095	475	.177	735	.317	1085	.527	1165	.727
600	385	.136	562	.255	875	.457	1300	.759	1390	1.04
700	450	.186	660	.347	1025	.622	1510	1.03	1620	1.42
800	510	.243	760	.454	1170	.812	1725	1.35	1840	1.86
900	570	.307	870	.575	1315	1.02	1960	1.70	2070	2.35
1000	635	.380	960	.710	1465	1.27	2150	2.11	2300	2.91
1100	700	.459	1037	.859	1610	1.53	2365	2.55	2525	3.52
1200	760	.547	1130	1.02	1750	1.82	2575	3.03	2760	4.19
1300	825	.642	1225	1.19	1875	2.14	2785	3.56	2980	4.91
1400	890	.744	1310	1.39	2040	2.48	3000	4.13	3215	5.70
1500	950	.855	1415	1.59	2190	2.85	3210	4.74	3440	6.54
1600	1010	.972	1500	1.81	2340	3.25	3425	5.40	3665	7.44
1700	1070	1.09	1590	2.05	2480	3.67	3635	6.09	3900	8.40
1800	1135	1.38	1705	2.30	2640	4.11	3850	6.83	4125	9.42
1900	1200	1.37	1790	2.56	2775	4.58	4050	7.61	4350	10.50
2000	1260	1.52	1875	2.84	2920	5.08	4275	8.44	4575	11.64
2100	1325	1.67	1875	3.13	3060	5.60	4425	9.30	4800	12.87
2200	1390	1.83	1970	3.43	3220	6.14	4690	10.21	5035	14.13
2300	1450	2.01	2150	3.75	3365	6.71	4900	11.16	5260	15.44
2400	1510	2.18	2250	4.08	3510	7.31	5100	12.15	5490	16.81
2500	1575	2.37	2340	4.43	3625	7.93	5325	13.18	5715	18.25
2600	1635	2.56	2425	4.79	3790	8.58	5525	14.26	5940	19.73
2700	1700	2.77	2520	5.17	3960	9.25	5740	15.38	6135	21.28
2800	1760	2.97	2610	5.56	4085	9.95	5950	16.54	6390	22.89
2900	1825	3.19	2715	5.97	4225	10.68	6125	17.74	6610	24.55
3000	1890	3.42	2800	6.39	4375	11.43	6365	18.99	6840	26.28

Two series of tests have been conducted using the magnetic fields. In the first series, performance was measured for a range of magnetic field strengths, while in the second series, a method was used for detecting arc rotation by examining swirl marks on an independently heated cathode.

Results of the first series are shown in Table 3. The propellant flow rate was held at a constant value (0.025 gm/sec) while the magnetic field strength, power level, and nozzle throat diameter were varied.

The first indications from these tests were as expected, that the arc voltage increased when a stronger magnetic field was applied. This voltage increase was accompanied with a visually more intense confinement of the exhaust plume toward the centerline. When comparing the various data it must be considered that the thruster performance depends also largely upon the electrode configuration used. The numerical results reported in the table have been averaged from various tests conducted in different periods of time using different electrode configurations. For this reason the values are only indicative of trends of performance. These preliminary findings will have to be substantiated through further testing and more conclusive results thereof will be reported when they become available.

For the second series of tests, the cathode was provided with an independent heater. Figure 6 shows a schematic cross-sectional view of the concept. A tungsten rod was inserted into the cathode which can be independently heated by a separate power supply so that the cathode can be brought close to its melting temperature prior to arc start-up. It was expected that, due to thermionic emission of the cathode, a more gentle start-up of the arc could be achieved. The first photograph in Figure 6 indicates that the electrode material begins to swirl as soon as the melting temperature of the tungsten is approached. This effect was already noted when only a moderate magnetic field was applied (e. g. , 1000 gauss). The swirl effect became more evident as arc current and magnetic field strength were increased as shown in the photographs 2 and 3, Figure 6. These practical demonstrations show that a very strong rotation of the arc plasma, in this case particularly in the cathode region, does indeed exist.

### 2.3 The Effect of Magnetic Interaction on the Thrust Measurement

As was reported in reference 1, it has been found that the magnetic field coils can interact with the steel walls of the vacuum chamber to produce an erroneous thrust reading. In the past, this has been compensated for by using a special steel plate which could be moved in the axial direction either toward or away from the coil until the effect vanished with the coil energized but the thruster not running. The interaction is due to the fact that the thruster is located off-center in the vacuum chamber so that the coil is closer to

TABLE 3

## THRUSTOR PERFORMANCE COMPARISON AT CONSTANT MASS FLOW AND DIFFERENT OPERATING CONDITIONS

Isp Sec	Thrust Grams	Throat Dia. Inches	Arc Press. mmHg	Magnetic Field Coll Tns Gauss	Volts	Amps	Pow. Input KW	Gas KW	$\eta_{eg}\%$	$\eta_{gk}\%$	$\eta_{eak}\%$	$\eta_{etk}\%$
3000	75	.437	36	0	44	1760	78	44	56	24	14	14
3080	77	.437	36	0	45	1580	71	51	68	22	15	15
3000	75	.437	38	4	42	1550	65	38	58	29	16	15
3000	75	.437	38	4	43	1490	65	37	57	29	16	15
4200	105	.375	58	0	46	2240	103	72	70	29	20	20
4000	100	.500	33	4	50	1820	91	58	64	31	21	20
5000	125	.375	55	0	52	2650	137	87	63	35	22	22
5150	129	.375	52	0	51	2660	136	86	63	37	23	23
5200	130	.625	19	4	62	2000	124	74	60	43	26	25
5800	145	.562	26	4	60	2130	128	82	64	48	31	30
6200	155	.375	50	0	54	3000	162	107	66	43	28	28
6000	150	.800	18	8	82	1900	155	83	54	52	28	27
6900	173	.375	49	0	57	3100	178	120	68	46	32	32
6600	165	.500	28	4	64	2370	152	99	65	54	35	34
6500	166	.750	19	8	85	2050	175	95	54	54	29	28
8000	200	.375	47	0	60	3400	204	140	69	56	38	38
8000	200	1.000	10	8	111	1910	212	135	64	57	37	36
8000	200	.812	22	8	85	2500	215	135	63	57	37	35
8000	200	.812	23	12	98	2110	208	120	59	64	37	35
8000	200	.812	23	16	105	1950	205	116	56	66	38	36

$H_2$  Propellant flow = .025 gm/sec

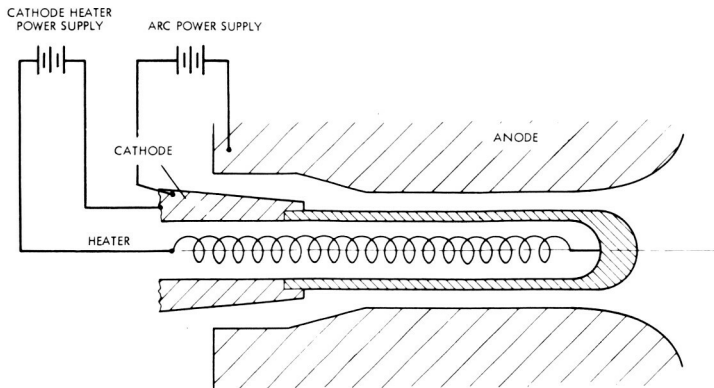
$\eta_{eg}$  = Thermal eff. = Gas KW/Electric KW arc  $\times 10^2$

$\eta_{gk}$  = Thrust eff. = Kinetic KW/Gas KW  $\times 10^2$

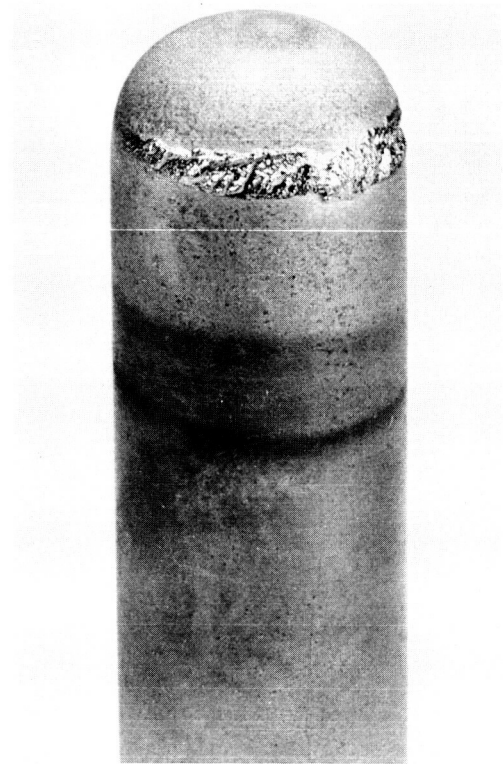
$\eta_{eak}$  = Overall eff. = Kinetic KW/Electric KW arc  $\times 10^2$

$\eta_{etk}$  = Total eff. (coil incl.) = Kinetic KW/Electric KW arc + coil  $\times 10^2$





Schematic of Cathode Heater



Light Swirl Effect at Moderate Magnetic Field



Increased Swirl Effect at Increased Magnetic Field



Heavy Swirl Effect at Strong Magnetic Field and Overheated Cathode

Figure 6. Cathode Heating Concept and Swirl Effect on Heated Cathodes

one wall. To avoid the time-consuming compensation procedure which had to be repeated each time the thruster configuration was changed, a thruster has been constructed with extended electrodes. Figure 7 shows a photograph of the thruster. The distance that the electrodes protrude is selected so that the magnetic field coils and the exhaust plume are located symmetrically with respect to the surrounding vacuum chamber walls.

To calibrate the thrust stand with this new device, the electrodes were short-circuited in the arc region and current values up to 3000 amps were passed through the thruster, producing a magnetic field larger than 6000 gauss (for the 16-turn coil). In this condition, no further parasitic thrust effect due to magnetic attraction of the tank walls could be found, and no further compensation of the thrust was necessary.

In addition to magnetic effects caused by the coil, there are magnetic effects due to current in the arc and possible current flows in the ionized gas surrounding the thruster. These effects are not properly duplicated when the thrust stand is calibrated as described. During tests of thermo-ionic thrusters, glow discharges usually appear on the outer housing of the thruster, indicating that external current flows are present. However, since the amount of current and the size of the current pattern isn't known, the importance of the error introduced to the thrust measurement cannot be estimated. Figure 8 shows the assumed current discharge pattern as it might occur when none or only weak magnetic fields are applied to the thruster. To assure that possible induced interactions of these discharge patterns with the tank walls will be negligible, it has been suggested that very large insulated tanks be used for future experiments. It is hoped that direct discharge phenomena from arc to tank can thereby be reduced. Very large vacuum tanks with low ambient pressures appear to be the only valid space simulation environment for the various arc thrusters now under study. However, it is felt that only actual space flight tests will completely answer the question. Figure 9 shows schematically the relative position of the exhaust plume to the tank wall, and the proposed dimensional relations for a large vacuum tank. It may become necessary to construct the entire vacuum tank from an insulating material to prevent current loops. It is intended to more qualitatively demonstrate parasitic interaction of the arc exhaust with the surrounding tank walls during the following program period.

#### 2.4 Tests with Deuterium

Some tests have been conducted using deuterium as the propellant as an initial phase of a test program to evaluate propellants other than hydrogen for thermo-ionic thrusters. Deuterium was selected for the first in the series because it has essentially the same properties as hydrogen except for the molecular weight. Since only one variable is changed at a time, it is hoped that the test results will be more meaningful to analyse the performance of thermo-ionic thrusters.

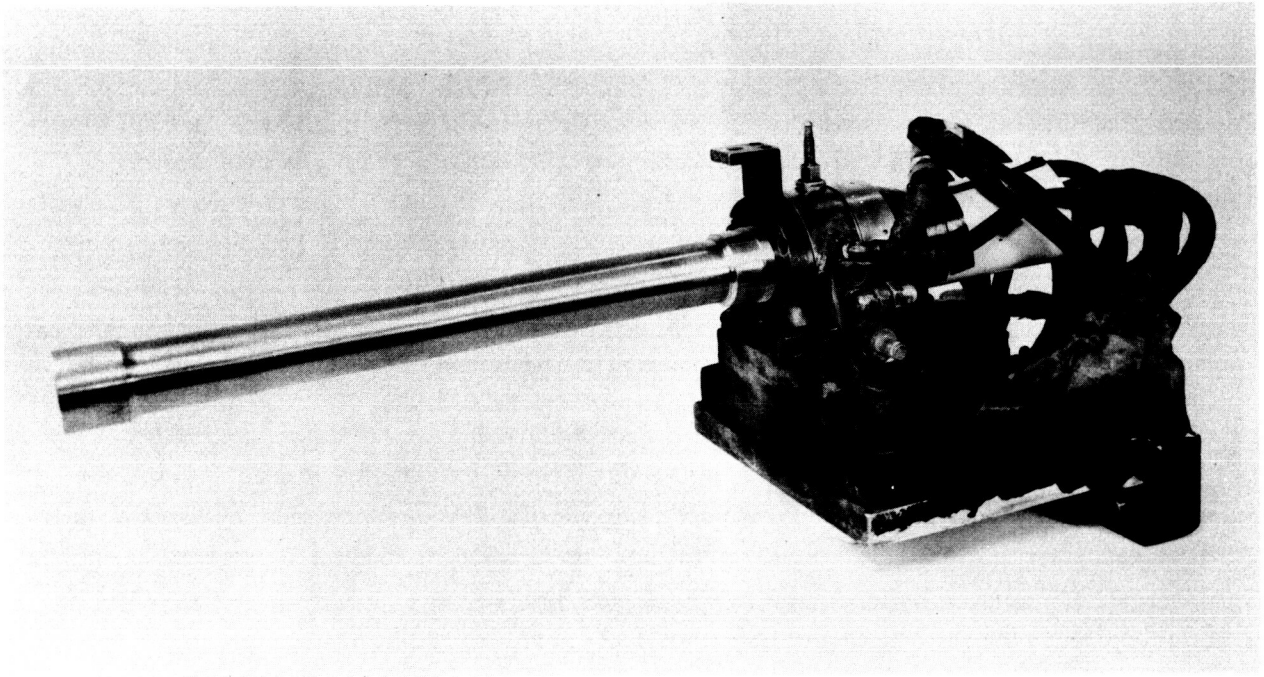
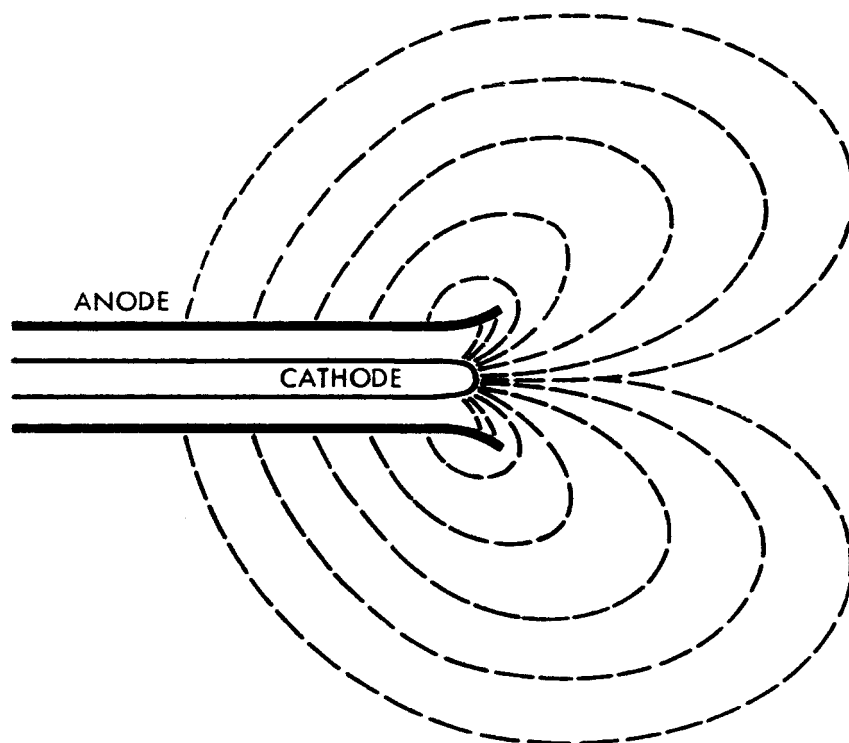


Figure 7. Experimental Thermo-Ionic Thrustor With Extended Electrodes



**Figure 8. Estimated Path of Current Discharge With Extended Electrodes  
at No or Weak Magnetic Field**

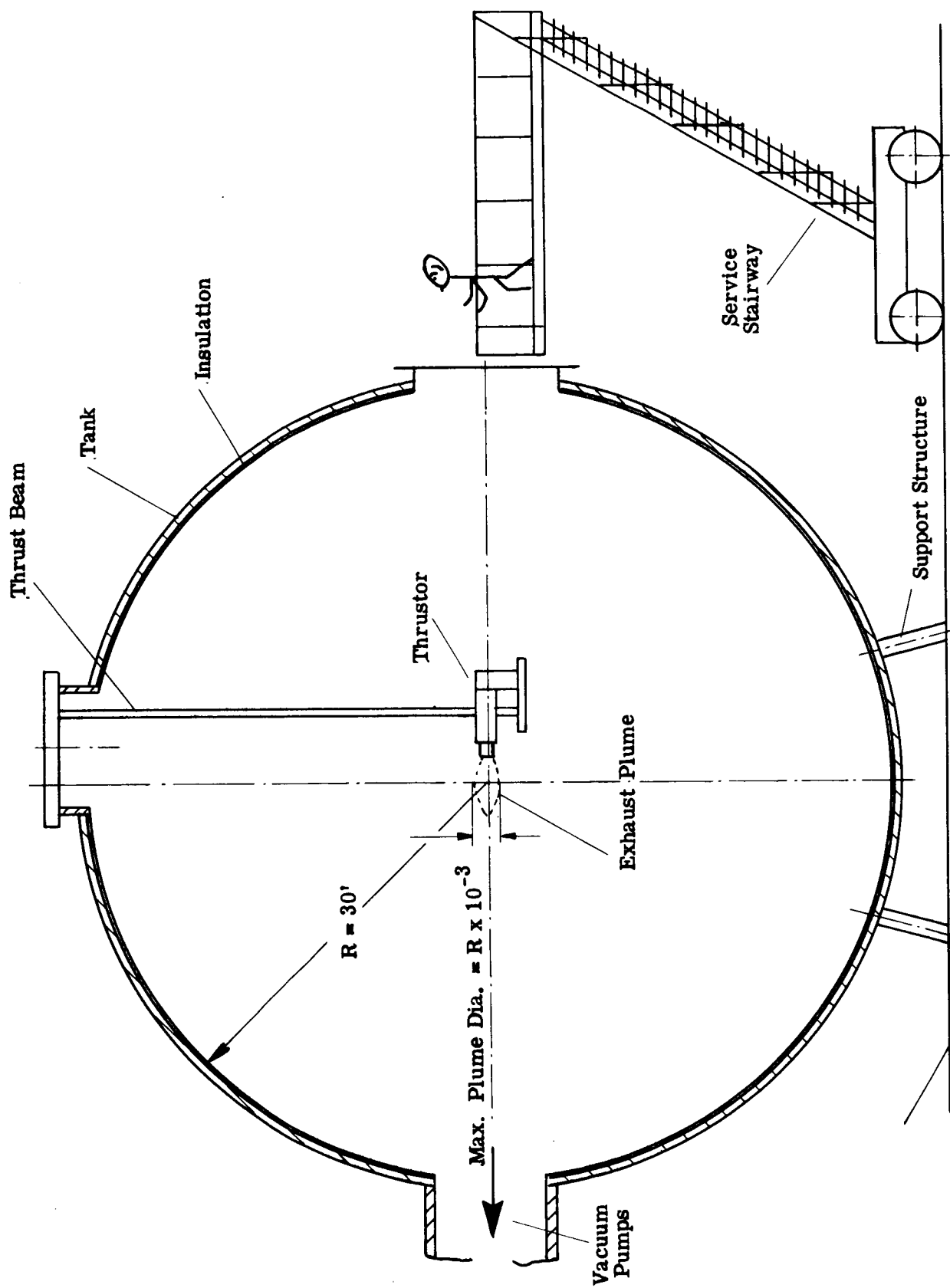


Figure 9. Proposed Enlarged Test Chamber

A large cylinder containing approximately 2 pounds of deuterium was obtained from the Los Alamos Laboratories through the cooperation of Dr. Thomas Stratton. A special flow circuit was installed on the thrust stand (critical orifice, etc.) to allow a precise weight flow calibration of the propellant flow rates (1-50 mg/sec) which were used during the testing.

It was decided to start up the engine with the regular Paschen Law technique using hydrogen as the starting gas. The special flow system permitted the introduction of deuterium gas as soon as the arc was established, while the hydrogen flow was gradually reduced at the same time through a manual throttling valve. Figure 10 shows a schematic diagram of the two flow circuits and is self-explanatory. During the preliminary testing it had been assured that the flow of hydrogen starting gas was eliminated by adding an extra precision manual cut-off valve in the hydrogen flow line as indicated in the sketch (Figure 10). The first experiments with deuterium gas proved to be quite similar to those when using hydrogen. No power fluctuations or instantaneous arc changes were noted. One difference between hydrogen and deuterium that was noticed was the change in the color of the jet. This difference is evident when the color of the arc starting gas, hydrogen (bright pink), changes to a more deep red and yellow when only deuterium is used. At first it was assumed that impurities in the deuterium gas storage cylinder could be the cause, but the deuterium supplier has assured us that the gas is of the highest purity obtainable.

It was also noted that the overall thruster operation with deuterium was nearly identical to that when hydrogen was used, but the kinetic efficiency was consistently higher. Table 4 presents a direct performance comparison of hydrogen and deuterium propellants at various levels of Isp and at propellant flow rates of 25 and 50 mg/sec. The comparative performance tests for hydrogen and deuterium have been made at test conditions matched as closely as possible. The electrode configuration was identical. An externally applied magnetic field obtained with a coil in series with the arc current was used. The lower arc chamber pressures for deuterium at identical Isp and mass flow are evidence of the higher molecular weight of this propellant. The comparison of the hydrogen and deuterium performance is interesting and deserves further investigation. The data as presented are quite accurately repeatable. However, there may exist parasitic effects in the arc discharge phenomenon which could influence these results. Tests will have to be repeated when these various parasitic phenomena are either understood and eliminated or found to be non-existent. Some specific tests to determine possible parasitic effects are planned for the next part of this research program.

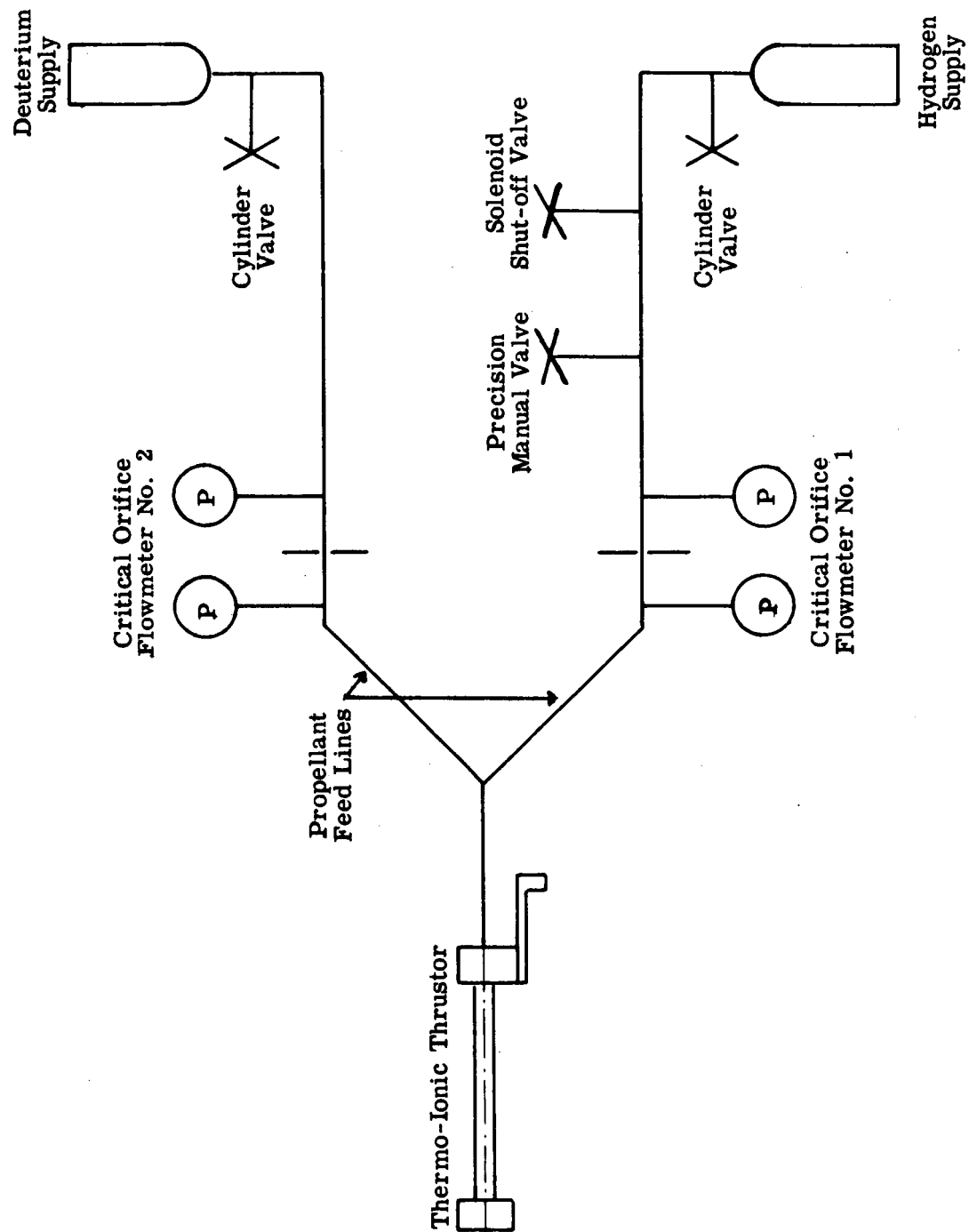


Figure 10. Schematic Diagram of Dual Propellant Flow System

TABLE 4

## PERFORMANCE COMPARISON OF HYDROGEN AND DEUTERIUM PROPELLANTS

Pro- pellant	Isp Sec	Thrust Grams	Mass Flow mg/sec	Arc Press. mmHg	Volts	Amps	Pow. Input KW	Gas KW	Efficiencies $\eta_{eg}\%$ $\eta_{gk}\%$ $\eta_{ek}\%$
H <sub>2</sub>	2000	100	50	34	82	950	78	46.0	59   20.9   12.2
H <sub>2</sub>	2000	100	50	35	80	1000	80	47.0	57   20.4   12.0
H <sub>2</sub>	2000	100	50	34	84	930	78	45.6	56   21.0   12.2
D <sub>2</sub>	2000	100	50	26	62	1090	68	38.4	56   25.0   14.1
D <sub>2</sub>	2000	100	50	27	65	1060	69	40.0	58   24.0   13.9
D <sub>2</sub>	2000	100	50	27	64	1075	69	38.8	56   24.2   13.9
H <sub>2</sub>	2000	50	25	23	61	886	54	24.5	45   19.6   8.9
H <sub>2</sub>	2000	50	25	22	58	850	49	24.0	49   20.0   9.8
H <sub>2</sub>	2000	50	25	23	59	900	53	25.0	47   19.2   9.0
D <sub>2</sub>	2000	50	25	19	46	936	43	19.8	46   24.2   11.1
D <sub>2</sub>	2000	50	25	19	47	935	44	20.2	46   23.7   10.9
D <sub>2</sub>	2000	50	25	18	45	910	41	19.3	47   24.9   11.7
H <sub>2</sub>	4000	100	25	24	82	1220	100	35.0	55   34.9   19.2
H <sub>2</sub>	4000	100	25	25	83	1230	102	55.0	54   34.9   18.8
H <sub>2</sub>	4000	100	25	25	84	1250	105	60.0	57   32.0   18.3
D <sub>2</sub>	4000	100	25	20	65	1290	84	45.5	54   42.2   22.9
D <sub>2</sub>	4000	100	25	20	63	1320	82	43.5	53   44.1   23.4
D <sub>2</sub>	4000	100	25	19	62	1305	81	44.0	54   43.7   23.7



### 3.0 CONCLUSIONS AND RECOMMENDATIONS

During this quarterly period the primary effort has been directed toward improving the performance of thermo-ionic thrusters and obtaining a better understanding of how the propellant mass is accelerated. The detailed performance of the thrusters is still not clearly understood. However, the following conclusions may be stated from the work reported herein.

1. Thermo-ionic thrusters can be scaled down in size (to as low as 5 KW) without a large loss in performance.
2. In the range of external magnetic fields tested, the overall performance obtainable with a thermo-ionic thruster does not depend strongly on the strength of the magnetic field; however, lifetime of the electrodes and voltage of operation is directly affected by the external magnetic field.
3. The use of a magnetic field results primarily in rotation of the arc and confinement toward the centerline of the exhaust plume.

These conclusions are based on test results and are not completely understood on an analytical basis. Further test work is needed to better define the importance of magnetic field strength, the choice of propellant, and interactions between external current flows and the vacuum chamber walls and residual ambient gases.

## REFERENCES

1. "Design and Development of a Thermo-Ionic Electric Thrustor," 1QS094-968, Interim Report, September 1964.
2. "Design and Development of a Thermo-Ionic Electric Thrustor," 2QS114-968, Interim Report, November 1964.
3. "Recent Progress in High Specific Impulse Thermo-Ionic Acceleration," AIAA Paper No. 65-96, New York, January 25-27, 1965.